Proceedings of the 9th World Congress on Mechanical, Chemical, and Material Engineering (MCM'23)
Brunel University, London, United Kingdom –August 06-08, 2023
Paper No. HTFF 164
DOI: 10.11159/htff23.164

Combined Natural Convection and Radiative Heat Transfer from a Horizontal Helical Coil Placed on the Ground and in Air: A Comparative Study

Gloria Biswal[1], Sukanta Kumar Dash[1]
[1]Indian Institute of Technology, Kharagpur
Department of Mechanical Engineering, Indian Institute of Technology, Kharagpur - 721302, India
gloria94@iitkgp.ac.in; sdash@mech.iitkgp.ernet.in

Abstract **-** The current work presents a comparative analysis of natural convection and radiation heat transfer from a solid isothermal helical coil either placed on the ground or suspended in the air. Numerical simulations are carried out in the range of Rayleigh number $\left(10^4 \le Ra \le 10^8\right)$, surface emissivity $\left(0 \le \varepsilon \le 1\right)$, geometrical parameters of the helical-coil, like diameter of the coil $\left(8 \le D/d \le 24\right)$, and pitch $\left(3 \le p/d \le 7.5\right)$. A graphic representation of the effects of geometrical parameters on heat transfer characteristics has been depicted, including average *Nu*, relative convection and radiation rates, and temperature contours. Radiation heat transfer is modeled using the S2S radiation model. A helical-coil in the air always has a higher average *Nu* than one on the ground. It is found that with an increase in *D/d*, the heat loss from the coil rises for all *p/d* and *Ra* because the coil opening area on either side of the helical coil expands, providing less resistance to the core flow. When the coil is on the ground, and when *D/d* varies from 8 to 24, the relative strength of Q_c rises by 2% and 1.07% for *p/d*=7.5 and 3 respectively at $Ra=10^4$.

Keywords**:** Natural convection, S2S Radiation model, Helical coil, Heat Transfer, Nusselt number

1. Introduction

Helical coils have been receiving much attention in the past few years due to its widespread usage in engineering and domestic applications. They are found to be used in nuclear reactors, electric room heaters, immersion water heaters, suspension systems for vehicles, etc. The reason helical coils are gaining popularity is because they have large heat transfer area, are compact, and, most significantly, their shape facilitates good mixing of the fluid across the interhelical spacings, which in turn raises the heat transfer coefficients [1]. Helical coils are generally manufactured at an extremely high temperature. Before being transported for industrial usage or further processing, they must be completely cooled down. Natural convection heat transfer is the viable method to cool the hot helical coils.

Ali [2] investigated the natural convection heat transfer from helical coils immersed in a water tank. Tests were conducted using two different tube sizes, 8 mm and 12 mm outer diameter, five various coil diameters, and up to five different pitch from 1.5 to 4 with 5 or 10 coil turns. According to their observations, the heat transfer coefficient for the 12 mm OD tube drops with length, while, the heat transfer coefficient for the 8 mm OD tube significantly increases with coil length. An experimental investigation was carried out by Prabhanjan et al. [3] to examine the heat transfer from helically coiled tubes housed in a big water bath by natural convection. They created an iterative prediction model that uses several characteristic lengths to assess the outer convection coefficients. Three different helical coils with different orientations; vertical and horizontal- have been the subject of experimental research by Xin and Ebadian [4]. The relationship between *Nu* and *Ra* has been correlated using several characteristic lengths. Moawed [5] presents an experimental analysis of steady-state natural convection heat transfer from uniformly heated helicoidal pipes that are oriented both vertically and horizontally. The findings demonstrated that for vertical helicoidal pipes, the overall Nusselt number rises as the ratio of coil-diameter to pipe-diameter (*D/do*), pitch to pipe-diameter (*p/d*o), and length to pipe-diameter (*L/do*) increases. The influence of various geometrical dimensions of helical-coil on natural convection heat transfer was reviewed by Heo and Chung [6] using mass transfer analogy concept. They identified that when the pitch-to-diameter ratio is less than 1.5, the preheating effect predominates, which lowers the Nusselt number, and at a pitch-to-diameter ratio of larger than 5 reduces the plume effect

from the lower turns. Biswal et al. [7], [8] numerically investigated the influence of helical-coil geometry (*D/d*, *p/d,* and *H/d*) on heat transfer characteristics when it is vertically suspended in the ambient air.

The main objective of this paper is to study the effect of *D/d*, *p/d*, ε, and *Ra* on the heat transfer characteristics when the coil is either suspended in air or lying on the ground. The natural convection from the outer surface of an isothermal helical coil with a wide range of geometrical parameters, however, has received very little attention despite its compact structure and widespread use, which is what inspired us to carry out this numerical study.

2. Physical Description of the Problem

Figure 1(b) displays an isothermal solid helical coil oriented horizontally in air and Fig. 1(c) displays the same coil lying on the ground. Here *D*, *H*, *p*, and *d* represent the coil diameter, coil height, pitch, and helical rod diameter respectively as illustrated in Fig. 1(a). An ambient air temperature (T_∞) and coil surface temperature (T_s) is taken as 400 K and 300 K respectively. The effect of radiation is included since the temperature difference between the coil and the ambient air is high. For comparison, it is proposed that the horizontal helical coil has a fixed total surface area (A). The overall coil-length and rod diameter (d) are taken as 0.01 m and 5 m, respectively. Since the surface area of the coil is constant, the characteristic length scale (L_c) is determined as the square root of this surface area i.e. $L_c = \sqrt{A}$ [9]. The numerical computations are performed in the following ranges of non-dimensional parameters: $8 \le (D/d) \le 24$; $3 \le (p/d) \le 7.5$; $10^4 \le Ra \le 10^8$; and $0 \le \varepsilon \le 1$.

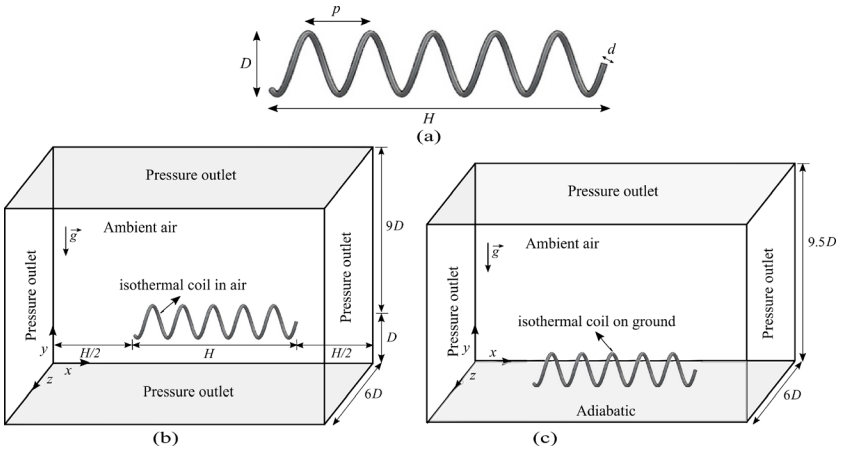

Fig 1: Schematic of computational domain; (a) helical coil geometry (b) coil suspended in air (c) coil lying on the ground.

3. Mathematical modeling of the problem

For the current study, we assume that the flow around the coil is three-dimensional, laminar, steady, and incompressible. The ambient fluid behaves as an incompressible ideal gas. The strength of velocity is feeble, so the effect due to viscous dissipation is neglected.

In this case, the governing system of equations are the following:

Continuity equation:

$$\nabla . \vec{\mathbf{V}} = 0 \tag{1}$$

Momentum equation:

$$\rho\left(\vec{\mathbf{V}} . \nabla\right)\vec{\mathbf{V}} = \rho\,\vec{\mathbf{g}} - \nabla P + \mu\left(\nabla^2 \vec{\mathbf{V}}\right) \tag{2}$$

Where, ρ, g, P, and μ are the fluid density, acceleration due to gravity, pressure, and dynamic viscosity respectively.

Energy equation:

$$\rho c_p \left(\vec{\mathbf{V}} . \nabla \right) T = k \left(\nabla^2 T \right) + s_h \tag{3}$$

where, s_h, c_p, k, and T are volumetric heat source due to radiation, specific heat, thermal conductivity, and Temperature respectively.

Equation of state:

$$P = \rho R T \tag{4}$$

3.1. Radiation Model

The radiation heat transfer from the helical coil has been assessed in the current study using the surface-to-surface (S2S) radiation model [10], [11]. The surface of the helical coil is considered to be gray, diffuse, and opaque. The air around the coil acts as a non-participating medium. Only the surface radiation from the coil is considered. Radiosity of a surface, b, comprises an emitted and reflected radiation and is represented at each participating surface as

$$J_b = E_b + (1-\varepsilon) \sum_{c=1}^{N} F_{bc} J_c \tag{5}$$

where J_b, E_b, J_c, ε, and F represent the radiosity of the surface b, emissive power of the surface b, and radiosity of the surface c, surface emissivity, and view-factor respectively.

These sets of equations can be expressed in matrix form as

$$KJ = E \tag{6}$$

Here K is an $N \times N$ matrix, J and E are the radiosity and emissive power vectors respectively. The radiosity values of the participating surface are obtained by solving Eq. (6) with ANSYS Fluent.

The net radiation heat flux leaving a surface, i, is defined as the difference between the radiosity flux (j_i) and the irradiation flux (g_i) falling on the surface, i, and is expressed as

$$q_{net.rad,i} = j_i - g_i = \frac{\varepsilon_i (e_{bi} - j_i)}{(1-\varepsilon_i)} \tag{7}$$

Where, e_{bi} is the black-body emissive flux and ε_i is the emissivity of the surface, i, which is provided as input while specifying the boundary conditions.

The source term, s_h, in the energy equation, Eq. (3) is calculated using Eq. (7) as [11]

$$s_h = -\nabla . q_{net.rad} \tag{8}$$

3.2. Boundary conditions

Coil surface:

$$T = T_s \ , \ u = v = w = 0 \tag{9}$$

Domain boundary (except the bottom surface for the coil placed on the ground):

$$P = P_{atm} \ \text{ or } \ P_{gauge} = 0, \ T = T_\infty \tag{10}$$

Here P_{atm}, P_{gauge} and T_∞ denotes the atmospheric pressure, gauge pressure, and temperature of the ambient respectively.

For bottom surface only when the coil is placed on the ground:

$$\frac{\partial T}{\partial n} = 0 \, ; \text{ Adiabatic wall condition} \tag{11}$$

We have assumed that fluid properties like thermal conductivity, dynamic viscosity, and specific heat are temperature-dependent because the temperature difference between the helical coil and the surrounding air is significant. The fluid properties are shown as quadratic function of temperature [7] and applicable for the temperature range of 250 K to 650 K:

$$c_p(T) = 0.103409\times10^{4} - 0.284887T + 0.7816818\times10^{-3}T^{2} - 0.490786\times10^{-6}T^{3} + 0.10777024\times10^{-9}T^{4} \quad (12)$$

$$k(T) = -2.276501\times10^{-3} + 1.2598485\times10^{-4}T - 1.4815235\times10^{-7}T^{2} + 1.75350646\times10^{-10}T^{3} - 1.06657\times10^{-13}T^{4} + 2.47663035\times10^{-17}T^{5} \quad (13)$$

$$\mu(T) = -9.8601\times10^{-7} + 9.080125\times10^{-8}T - 1.1763575\times10^{-10}T^{2} + 1.2349703\times10^{-13}T^{3} - 5.7971299\times10^{-17}T^{4} \quad (14)$$

4. Numerical methodology

We have solved the governing equations (1)-(4), along with the imposed boundary conditions (9)-(11), using finite volume-based algebraic multi-grid (AMG) solver of Ansys FLUENT-15. For the pressure-velocity coupling, the SIMPLE algorithm is used, while second-order upwind schemes are used for discretizing convection terms in momentum and energy equations. The PRESTO (PREssure STaggering Option) scheme is used to discretize the pressure. The density, pressure, momentum, energy, and body force terms have an under-relaxation factor of 1, 0.4, 0.4, 1, and 1, respectively. The scaled residuals were set to 10^{-8} for the energy equation and 10^{-5} for all other equations. The convergence of the average Nusselt number (Nu) up to three decimal places has been examined. A previous work by the author [12] provides detailed information on how numerical methodology was implemented.

4.1. Domain and grid sensitivity analysis

It was necessary to perform the domain independence analysis to establish that the computational results were not affected if the computational domain size is altered. For this, a particular case of helical coil i.e. D/d=8, p/d=3, and ε=0.1 at Ra=10^4 was selected for carrying out the simulations. The dimensions of the domain were varied between 1.5H to 2.5H, 4D to 8D, and 6D to 14D for domain length, width, and height respectively. The average Nu is not substantially changing beyond a domain size of 2H*6D*10D, as indicated by Table 2. Therefore, for all of our numerical simulations, the 2H*6D*10D domain size was maintained.

Table 2: Effect of domain size on average Nu for p/d=3, D/d=8, H/d=60 and ε=0.1 at Ra=10^4

Domain size (length*width*height)	1.5H*4D*6D	1.75H*5D*8D	2H*6D*10D	2.25H*7D*12D	2.5H*8D*14D
Average Nu	22.870	23.352	23.633	23.701	23.719

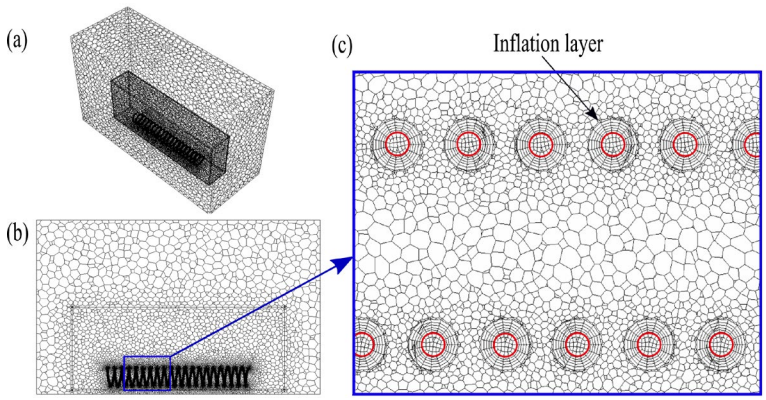

Fig 2: Cells arrangement in the domain; (a) isometric view, (b) transverse sectional view, and (c) enlarged view close to the coil

We are aware that the gradient of temperature and velocity is particularly steep close to the helical coil surface. Therefore, we need to build more fine mesh in that area to accurately capture the flow and heat transfer characteristics. Similarly, a coarse grid is used in the computational domain for regions far from the coil as illustrated in Fig 2. Grid sensitivity test must be done before running the final simulations to ensure that the numerical results are independent of the size of the cell. From Table 3, it can be marked that the number of optimal cells for a specific case of the current study at p/d=7.5, D/d=8, and ε=0.1 at Ra=10^4 was found to be 12.26×10^5.

Table 3: Variation of average Nu with number of grids for p/d=7.5, D/d=8, and ε=0.1 at Ra=10^4

No. of grids $\times10^5$	6.74	8.01	9.15	12.26	15.31
Average Nu	40.563	39.878	38.453	37.578	37.519

4.2. Validation

The numerical model of the present study is verified by simulating natural convection over a horizontal helical coil for which experimental results [4] are readily available. We have considered a horizontal helical coil with a diameter of 259 mm, 5 number of turns, rod diameter of 25.4 mm, and a pitch of 62.5 mm. As seen in Fig, 3, the present numerical model has fairly anticipated the experimental results.

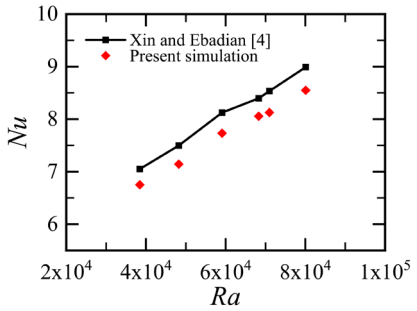

Fig 3: Comparison of Nu between the present numerical findings and the experimental results of Xin and Ebadian [4]

5. Results and Discussion

In this part, numerical simulations have been carried out to illustrate the effect of p/d, D/d, Ra, and ε on average Nu and the relative contributions of convective and radiative heat transfer. This is followed by the delineation of thermal contours, which are very helpful for understanding flow and heat transfer characteristics.

5.1. Effect of emissivity on heat transfer

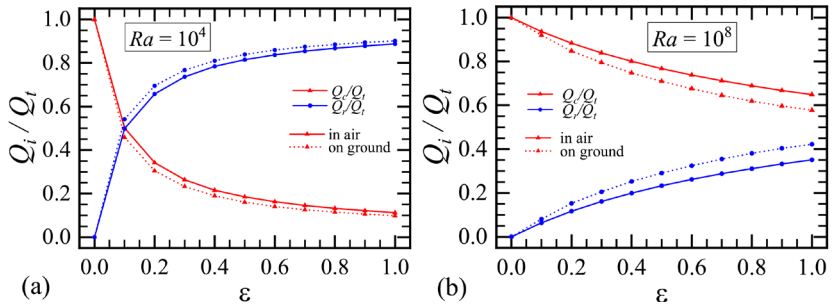

Fig 4: Comparison of convection and radiation strength with ε for p/d=3, and D/d=8 at (a) Ra=10^4 and (b) Ra=10^8

Figure 4 shows the variation of emissivity (ε) on convective heat transfer (Q_c) and radiative heat transfer (Q_r) for a horizontal helical coil suspended in the air as well as for helical coil lying on the ground as a function of its Rayleigh number (*Ra*). The solid line in the entire paper depicts the numerical outcomes when it is freely suspended in the air and the dotted line is for the coil when it is lying on the ground. From Fig 4(a) and 4(b), we can see that the relative strength of Q_c diminishes whereas the relative strength of Q_r increases with ε for all *Ra*. As long as *Ra* remains constant and ε increases, Q_r will rise without changing Q_c because ε does not have any effect on Q_c. Furthermore, an increase in overall heat transfer (Q_t) will result from a rise in Q_r. Consequently, the relative strength of radiation increases with the increase in ε, while the relative strength of convection decreases.

It can be noted that for all *Ra* and over the entire range of ε, the strength of Q_c for a solid helical coil in the air is marginally higher than that when it is lying on the ground because the bottom surface which intersects the ground cannot lose heat effectively due to the presence of the ground. At low $Ra=10^4$, the curves of the relative strength of Q_c and Q_r intersect at an ε of 0.1 and 0.08 for the coil in the air and on the ground respectively. Whereas such a cross-over point does not occur at high $Ra=10^8$, because the strength of buoyancy force is high, so, the convection mode of heat transfer prevails over the radiation mode.

5.2. Average Nusselt Number

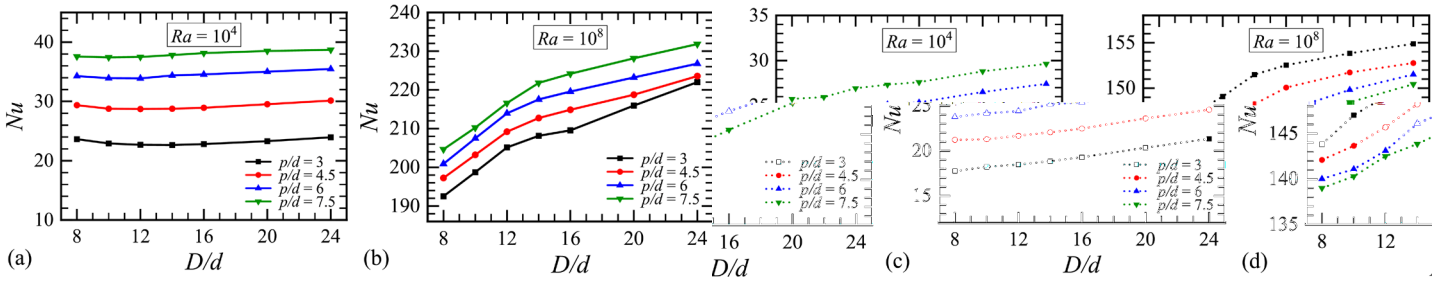

Fig 5: Average *Nu* with *D/d* and *p/d* at (a) $Ra=10^4$ (air), (b) $Ra=10^8$ (air), (c) $Ra=10^4$ (ground), and (d) $Ra=10^8$ (ground)

Figure 5(a) and 5(b) illustrate the comparison of average Nusselt number (*Nu*) with *D/d* as a function of *p/d* for $Ra=10^4$ and $Ra=10^8$ respectively for the case when the coil is suspended in air and Fig. 5(c) and 5(d) shows the average *Nu* for $Ra=10^4$ and $Ra=10^8$ respectively when the coil is lying on the ground. It can be highlighted that for all *Ra* and *p/d*, the average *Nu* rises with *D/d*. This phenomenon can be explained by the fact that as *D/d* rises, the coil opening area on either side of the helical coil expands, providing less resistance to the core flow. This allows more heat to be removed from coil surfaces as the air flow rate through the core increases.

When the coil is in air, the thermo buoyant flow penetrates from the two sides of the coil as well as the lower side of the helical coil, across the inter-helical spacing. The inter-helical gap between the turns expands as *p/d* increases from 3 to 7.5. When *p/d* increases, fresh air flows easily over the helical turns, dissipating more heat and causing *Nu* to rise for all *Ra*. Due to the presence of the ground, the natural convection plume emerging from the bottom of the coil is impaired, while in air, it proceeds unhindered from the bottom to the top. As a result, we observe that *Nu* is higher when the coil is in the air than when it is on the ground. At high $Ra=10^8$, the strength of buoyancy force is more as compared to $Ra=10^4$, so the flow rate increases, thereby increasing the *Nu*. But at the same time, with increase in *p/d*, the horizontal length of the coil increases at a fixed *D/d*. So, the fast-moving ambient air is unable to penetrate fully into the center of the core region. So, the average *Nu* decreases with increase in *p/d*.

5.3. Heat transfer contributions

Figure 6 shows the comparison of the relative strength of Q_c and Q_r around the helical coil when it is in the air (top row) and on the ground (bottom row) as a function of *D/d*, *p/d*, and *Ra* at ε=0.1. The relative strength of Q_c rises with *D/d* for all *p/d* and *Ra* whereas the relative strength of Q_r declines. It can be marked that the convection heat transfer is more

when the coil is suspended in the air as compared to when it is lying on the ground for all *Ra*. Q_r contributes to the total heat transfer in a complementary manner to convection heat transfer.

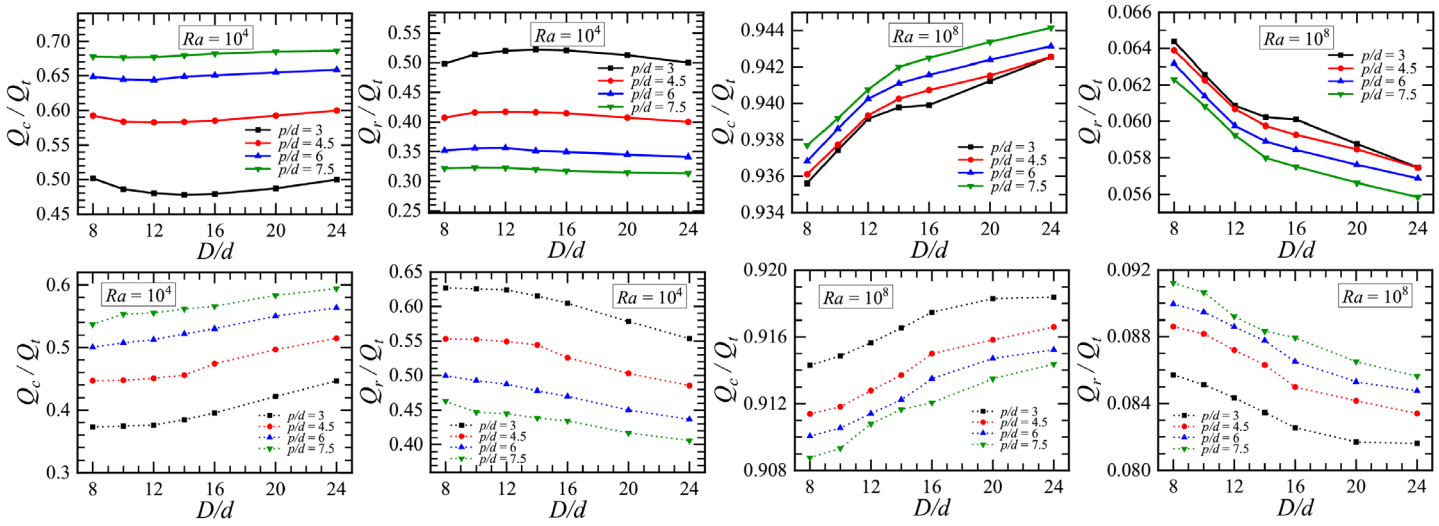

Fig 6: Relative strength of Q_c and Q_r with *D/d* at various *p/d* and *Ra* when coil is in air (top row) and on ground (bottom row)

At *Ra*=10^4, with rise in *p/d*, the strength of Q_c rises for both the coil in the air and on the ground. When the coil is on the ground, and when *D/d* varies from 8 to 24, the relative strength of Q_c rises by 2% and 1.07% for *p/d*=7.5 and 3 respectively at *Ra*=10^4. However, at *Ra*=10^8, with the increase in *p/d*, the relative strength of Q_c rises with *p/d* in the air but declines when it is on the ground.

5.4. Thermal field

Figures 7(a) and 7(b) portray the effect of *D/d* and *p/d* on the temperature contour for the coil in air and on the ground respectively at *Ra*=10^4. At low *D/d* and *p/d*, the plume temperature is very close to that of the coil, inside the core. The coil surrounding region is noticeably red (hot), indicating that the ambient temperature is close to the coil temperature. The ambient air is drawn into the center of the coil, but it does not effectively remove heat from the hot coil surface, leaving the core area hot and this is evidently observed in the case of *D/d*=8. When the coil is in the air, the thermal plume develops well from the bottom and goes to the upper portion. But when it is on the ground, the ground creates obstacles and so, the development of the plume is impaired and heat loss is comparatively less.

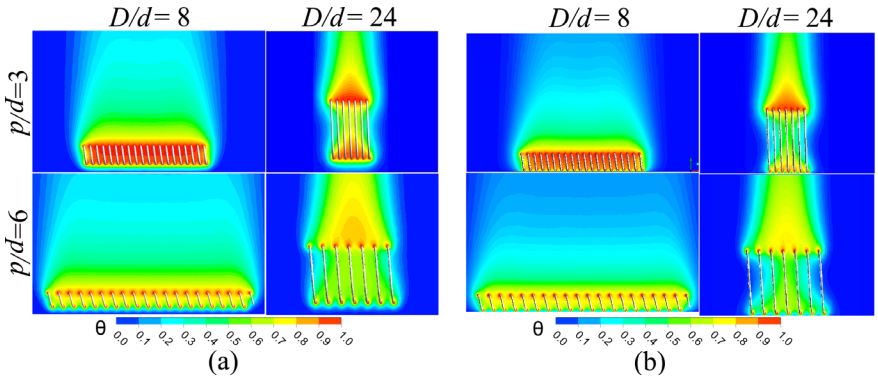

Fig 7: Temperature contours for different *D/d* and *p/d* at *Ra*=10^4 (a) in air (b) on ground

6. Conclusion

In the current study, the effect of D/d, p/d, Ra, and ε on natural convection and radiation heat transfer from the coil on the ground and suspended in air have been analyzed numerically. Some of the key findings are summarised below:

(a) The relative strength of Q_c decreases and Q_r increases with emissivity for all D/d, p/d, and Ra.
(b) The average Nu and the heat loss from the coil increase with the rise in D/d for both the coil in air and on the ground.
(c) At $Ra=10^4$, the average Nu and Q_c rise with p/d from 3 to 7.5 for both the coil in air and on ground. When the coil is on the ground, and when D/d varies from 8 to 24, the relative strength of Q_c rises by 2% and 1.07% for p/d=7.5 and 3 respectively at $Ra=10^4$.
(d) At $Ra=10^8$, the average Nu and Q_c decrease with a rise in p/d for the coil on the ground. Whereas, in the air, it increases with p/d.
(e) The heat loss from the coil is more when it is in the air as compared to the coil on the ground because the development of the thermal plume is hindered due to the presence of the ground.
(f) The present work helps the readers to gain a deeper understanding of heat transfer and fluid flow from the visualization of the contours that have been presented for various situations.

References

[1] M. Delgado, Y. A. Hassan, and N. K. Anand, "Experimental flow visualization study using particle image velocimetry in a helical coil steam generator with changing lateral pitch geometry," *International Journal of Heat and Mass Transfer*, vol. 133, pp. 756–768, 2019.

[2] M. E. Ali, "Experimental investigation of natural convection from vertical helical coiled tubes," *International Journal of Heat and Mass Transfer*, vol. 37, no. 4, pp. 665–671, 1994.

[3] D. G. Prabhanjan, T. J. Rennie, and G. S. V. Raghavan, "Natural convection heat transfer from helical coiled tubes," *International Journal of Thermal Sciences*, vol. 43, no. 4, pp. 359–365, 2004.

[4] R. C. Xin and M. A. Ebadian, "Natural convection heat transfer from helicoidal pipes," *Journal of Thermophysics and Heat Transfer*, vol. 10, no. 2, pp. 297–302, Apr. 1996.

[5] M. Moawed, "Experimental investigation of natural convection from vertical and horizontal helicoidal pipes in HVAC applications," *Energy Conversion and Management*, vol. 46, no. 18–19, pp. 2996–3013.

[6] J. H. Heo and B. J. Chung, "Influence of helical tube dimensions on open channel natural convection heat transfer," *International Journal of Heat and Mass Transfer*, vol. 55, no. 11–12, pp. 2829–2834, May 2012.

[7] G. Biswal, S. Rath, and S. K. Dash, "Natural convection and radiative heat transfer from constant surface area vertical helical coils: Effect of pitch and diameter," *International Communications in Heat and Mass Transfer*, vol. 141, p. 106578, 2023.

[8] G. Biswal, S. Rath, and S. K. Dash, "Effect of Surface Radiation on Natural Convection Heat transfer from a Helical Coil," in *Proceedings of the 26thNational and 4th International ISHMT-ASTFE Heat and Mass Transfer Conference December 17-20, 2021, IIT Madras, Chennai-600036, Tamil Nadu, India*, Begel House Inc., 2021.

[9] M. M. Yovanovich, "On the effect of shape, aspect ratio and orientation upon natural convection from isothermal bodies of complex shape," *ASME HTD*, vol. 82, pp. 121–129, 1987.

[10] A. Fluent, "15.0 User Guide, November 2013," *ANSYS Inc., South pointe, Canonsburg*.

[11] V. Karlapalem and S. K. Dash, "On the enhancement of natural convection heat transfer with multi-branching fins," *International Journal of Thermal Sciences*, vol. 183, Jan. 2023.

[12] G. Biswal, S. Rath, and S. K. Dash, "Natural convection and radiative heat transfer from constant surface area vertical helical coils: Effect of pitch and height," *Journal of Thermal Science and Engineering Applications*, vol. 15, no. 3, p. 031005, 2023.